Elastic bands for nonholonomic car-like robots : algorithms and combinatorial issues.

Hazem Jaouny, M. Khatib, Jean-Paul Laumond

CENTRE NATIONAL DE LA RECHERCHE SCIENTIFIQUE

LABORATOIRE D'ANALYSE ET D'ARCHITECTURE DES SYSTEMES

ELASTIC BANDS FOR NONHOLONOMIC CAR-LIKE ROBOTS : ALGORITHMS AND COMBINATORIAL ISSUES

H. JAOUNI, M. KHATIB, J.P. LAUMOND

LAAS REPORT 97477

DECEMBER 1997

Elastic bands for nonholonomic car-like robots: algorithms and combinatorial issues

H. Jaouni, M. Khatib, J.-P. Laumond
{hazem,maher,jpl}@laas.fr

LAAS-CNRS
7, Avenue du Colonel Roche, 31077 Toulouse Cedex 4 France

Paper submitted to WAFR'98

Abstract

This paper presents a dynamic structure allowing to enrich any nonholonomic motion planner for car-like robots with the capacity of reactiveness to environment changes. It is based on a pavement of paths by star shaped domains computed in the singular metric of the car-like robot. The algorithms to build such pavements are presented and their complexity is analyzed. We then introduce an optimization routine consisting in following the negative gradient of an energy function, the energy being the result of a combination of repulsive forces (due to obstacles) and attractive forces (tending to shorten the path). The key point of the approach is to consider the configuration space as a metric space equipped with the nonholonomic metric.

Applications to nonholonomic path planning including reactivity to moving obstacles are presented.

1 Elastic bands and nonholonomic metrics

About five years ago, Quinlan and Khatib [9] proposed a dynamic trajectory modification concept called the elastic band allowing to maintain a permanent flexible and deformable path between an initial and a final robot configuration. The key point of the concept lies on a pavement of the path with collision-free balls, whose size and shape present a simplified and practical image of the free space around the path. The sequence of balls that cover the path is called a bubble band. Applying contraction forces between bubbles and repulsion forces due to the obstacles transforms the bubble band into a elastic band. Among the possible applications of this concept let us mention the reactive control (allowing to account for environment changes during execution phase) and path optimization.

Elastic bands are wholly built on distance functions. They were first developed for holonomic robots where the metric space associated to shortest paths is simply the Euclidean space. In order to extend the bubble band to a nonholonomic robot, the problem of shortest paths should be resolved and the associated distances, between configurations and between a configuration and an obstacle, should be found.

The problem is solved for pointwise car-like robots. Reeds and Shepp [10] established a sufficient family that contains the shortest paths (from a configuration to a configuration) for such a robot. This family was refound and refined using control theory simultaneously by Sussmann and Tang [13] and by Boissonnat, Cerezo and Leblond [3]. The metric space associated to this set of shortest paths was established by Souères and Laumond [12] through

the partition of the configuration space into classes, each containing a single type of paths. Finally, the distances to points and segments in the plane were resolved, respectively, by Souères, Fourquet and Laumond [11] and by Vendittelli and Laumond [14].

Consequently, a bubble band for the car-like robot has been developed in [5] where the bubbles are balls in the corresponding metric space. This lead to a more general definition of the bubble band concept [6].

The interest of the bubble band (and the associated elastic band) lies in a simple combinatorial way to represent a given path among the obstacles surrounding it: the optimization routines are all the more efficient as the length of the sequence of bubbles is short.

In this paper we propose to replace the balls by "stars". A configuration being given, a star is the set of configurations which are reachable by an shortest path that does not intersect the obstacles. After introducing necessary definitions, we present an algorithm to compute the pavement of a path with stars and we compare its complexity with respect to the pavement with balls. It appears that, in the worst case of the parking task, both pavements have the same (optimal) complexity, while in the average cases, the pavement with stars is much less expensive than the pavement with balls. Finally, we show how to transform such a pavement with stars into an elastic band and we present experimental results dealing with nonholonomic path planning including reactivity to moving obstacles.

2 Bubble bands: definitions

The basic idea of the bubble band method is the pavement of an arbitrary path by a finite sequence of subsets in the configuration space. In order to guarantee the feasibility of the path, these subsets should verify several properties [8, 6]. The following definitions sum up these properties. The configuration space of the robot is a manifold $\mathcal{M}$. $\mathcal{O} \subset \mathcal{M}$ represents the union of obstacles.

Definition 2.1. Let $\mathfrak{O}(\mathcal{M})$ be a family of open subsets in $\mathcal{M}$ such that for all open subset $\mathcal{A}$ of $\mathcal{M}$, for all configuration P in $\mathcal{A}$, there is an element $\mathcal{B}$ in $\mathfrak{O}(\mathcal{M})$ that verifies:

- $\mathcal{B} \subset \mathcal{A}$ (*non-collision condition*),
- $P \in \mathcal{B}$ (*cover condition*),
- $\forall\, Q \in \mathcal{B}\ \exists$ a admissible path $\gamma(P, Q) \subset \mathcal{B}$ joining P to Q (*accessibility condition*).

$\mathfrak{O}(\mathcal{M})$ is called a set of *bubbles*. $\mathcal{B}$ is then a bubble whose *center* is P.

Definition 2.2. A *bubble band* joining an initial configuration $P_0 \in \mathcal{M}$ to a final configuration $P_1 \in \mathcal{M}$ is a finite sequence of bubbles $\{\mathcal{B}_i, i = 1, \ldots, n\}$ such that:

- All the bubbles $\mathcal{B}_i$ belong to the *free space*: $\mathcal{M} - \mathcal{O}$.
- $\mathcal{B}_i \cap \mathcal{B}_{i+1} \neq \emptyset\ \forall i = 1, \ldots, n-1$.
- P_0 is the center of $\mathcal{B}_1$ and P_1 is the center of $\mathcal{B}_n$.

Since we are interested in car-like robots, we will restrict our discussion to the manifold $\mathbb{R}^2 \times \mathcal{S}^1$ which represents the configuration space of such robots. This manifold has a metric structure compatible with the shortest paths feasible by these robots [12]. This metric is denoted by d_{RS}; it has been proved to be equivalent to the Euclidean one. Then the balls issued from it (see Figure 1) form a set of bubbles that verifies the conditions of definition 2.1. Such a bubble is then defined by a center C and a radius d_C corresponding to the length of

the shortest path leading the car-like robot to a contact with an obstacle; they are denoted by $\mathcal{B}(C, d_C)$. Distance computation in this framework is addressed in [14]. A bubble band was developed that uses these bubbles for pointwise and circular car-like robots [5].

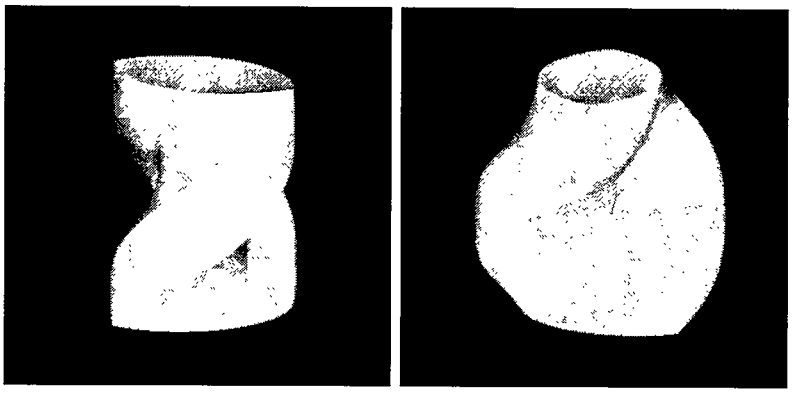

Figure 1: *Balls in the car-like robot metric*

In this paper we present another set of bubbles. These bubbles are also define by a center. Each bubble is defined to be the set of configurations directly reachable from its center by shortest paths. This set incorporates thus more information about obstacles than the previous one, which will lead to a better representation of the free space and thus to a more efficient bubble band.

Definition 2.3. Let C be a configuration of the free space. The *star* centered at C is the set of configurations that can be reached from C by shortest paths that does not intersect $\mathcal{O}$. It is denoted by $\mathcal{E}(C)$.

Figure 2 from [4] shows an example of the boundary of a star: in this example the obstacle is reduced to a straight line segment. This segment appears as a rectangular domain in the configuration space. The center of the star is the configuration $(0, 0, 0)$. The star is an unbounded domain whose (infinite) borders are truncated at some given distance from the origin for display purpose. The color of the various patches corresponds to the type of the shortest paths reaching the boundary.

The stars clearly verify the hypothesis of Definition 2.1: they are bubbles. Moreover, any collision-free shortest path starting at some some configuration C ends at a configuration belonging to $\mathcal{E}(C)$. Therefore, for any C, the star $\mathcal{E}(C)$ contains the ball $\mathcal{B}(C, d_C)$. As a consequence, the minimal number of stars necessary to cover an arbitrary path in a arbitrary environment is always lesser than the minimal number of necessary balls.

In fact we will show later that the maximal complexity of both bubble bands which corresponds to the number of bubbles that compose them and thus to the number of primitive operations necessary to join both ends is the same. Nevertheless, the mean complexity is lesser in the case of star bubbles because of the above corollary.

Throughout this paper, *ball band* designs the bubble band where the bubbles are balls of the metric space and *star band* the bubble band that uses the stars instead.

3 Pavements: algorithms and complexity

The starting point of the bubble band is an arbitrary collision-free path that joins a starting configuration to a goal configuration in $\mathbb{R}^2 \times \mathcal{S}^1$. This path is not necessarily feasible by the car-like robot. It may be computed by any (holonomic) motion planner.

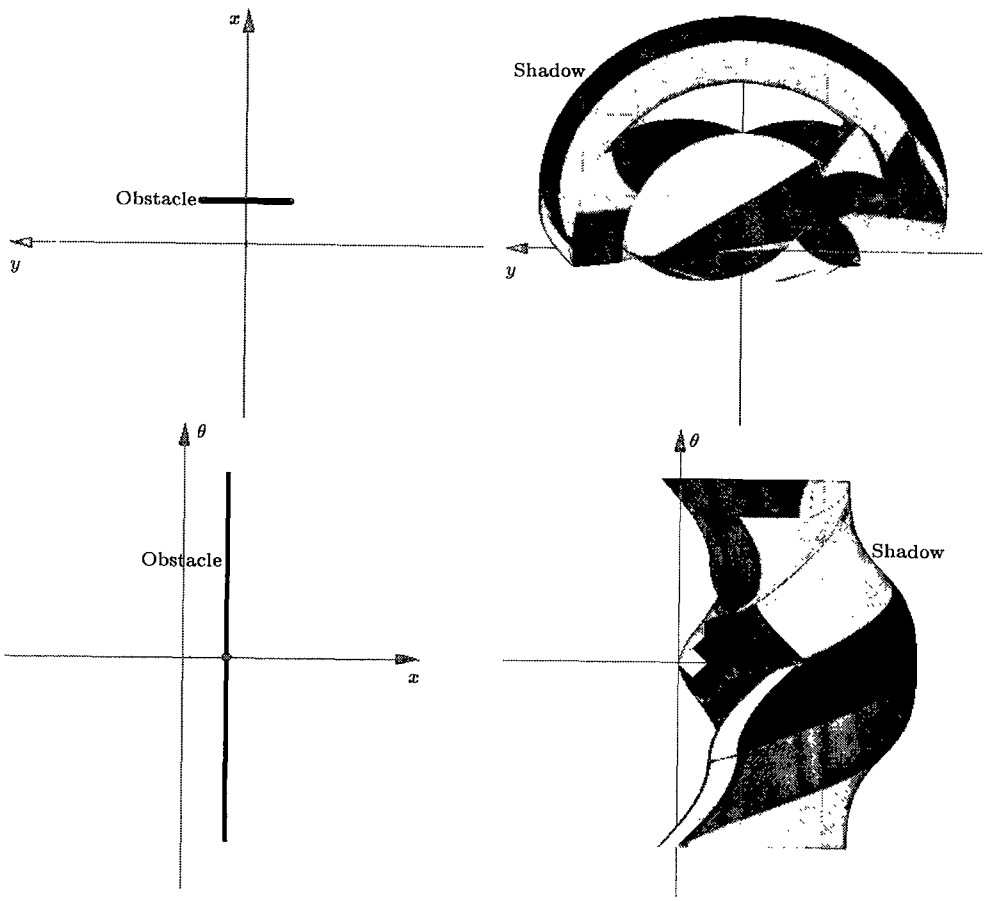

Figure 2: *Boundary of a star for a segment located near the origin.*

Let $\sigma : [0, \ell] \longrightarrow \mathbb{R}^2$ be such a path parameterized by arc length. ℓ is then the length of the path. We suppose that the obstacles are polygons in the plane and we note n the number of line segments that compose the boundaries of these obstacles. The robot is assumed to be a polygon.

Pavement by balls: In order to cover the path σ by a sequence of balls, two operations are necessary. The first one computes the distance from a given configuration to obstacles, noted $\text{dis}_{\mathcal{O}}$ and used to determine the size of the balls. This distance is taken to be the minimum of the n distances to the line segments that compose the set of obstacles. Computing the shortest path distance for a polygonal robot from a configuration to a straight line segment is still an open problem. The procedure we use in practice considers obstacles grown by the radius of the smallest circle enclosing the robot. It is then based on the results appearing in [14] and giving the shape of the shortest path for a pointwise car-like robot to either a point or segment; the distance to arcs of circles will be developed in an appendix in the final version of the paper.

The second operation is the distance d_{RS} between configurations associated to shortest paths. It is used to check the overlapping of consequent balls and thus to maintain the connectivity of the band. This second distance requires a constant time and is independent of both ℓ and n.

The pavement of the path σ by balls has been introduced in [5]. We start with the path σ.

This path is firstly sampled into a sequence of configurations. The number of the resulting configurations, noted l, is proportional to the length of the both, ℓ, and the resolution of the sampling. Then the first bubble is defined to be the greatest ball centered on the first configuration of the sequence. The sequence is then spanned until the last configuration still belonging to the last constructed bubble is reached. This configuration is thus taken to be the center of the following bubble which also has the maximum size. The previous step is repeated till the goal (or last) configuration is found to be in a bubble. A final ball is created around it. Figure 4 shows the pavement covering the path of Figure 3; the drawings correspond to the projection of the (3-dimensional) balls onto the plane.

Let b be the number of balls that compose the created band. The distance $\text{dis}_{\mathcal{O}}$ was used b times to determine the size of these balls while the distance d_{RS} was used $l-1$ times for the inclusion test. The complexity of this operation is then $O(l+nb)$.

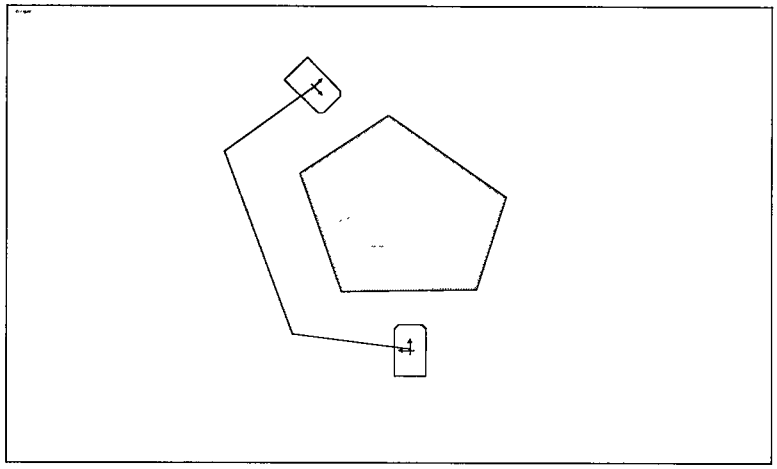

Figure 3: *Initial path.*

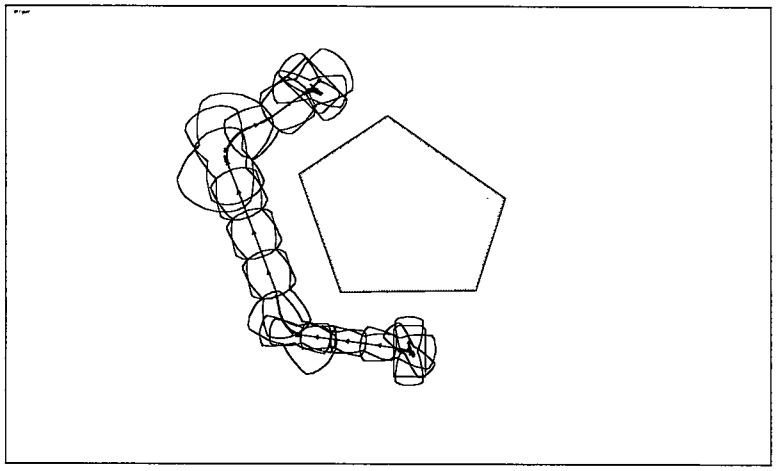

Figure 4: *Pavement with balls*

Pavement by stars: This pavement requires the answer to the question: 'is a given configuration "visible" from a starting one ?', i.e. 'is the shortest path between them collision-free ?' To answer this question we use the collision-checker described in [7]. It works for polygonal robot and its complexity is $O(n)$.

A pavement by stars can be computed with the same algorithm as the pavement by balls. Starting from the initial configuration, we search for the first configuration on σ which is not visible; then the configuration before becomes the center of a new star. The complexity of the algorithm is then $O(nl)$. Usually, $l \gg b$ and the complexity of this algorithm is much worse than the first one.

A better algorithm may be devised by using the inclusion of $\mathcal{B}(C, d_C)$ in $\mathcal{E}(C)$. It is composed of two steps. In the first one, we construct a ball band. Then the second step consists in spanning this band and in replacing the balls by stars. Whenever two stars are connected (i.e. the center of the first is in the second) all the intermediate bubbles are removed. The first step has the same complexity as the pavement by balls. The second step has a complexity equal to $O(nb)$. Finally, the total complexity remains $O(l + nb)$.

Figure 5 shows the result of the algorithm: four stars are sufficient to cover the initial path; the first four configurations appearing in the figure are the centers of the four stars.

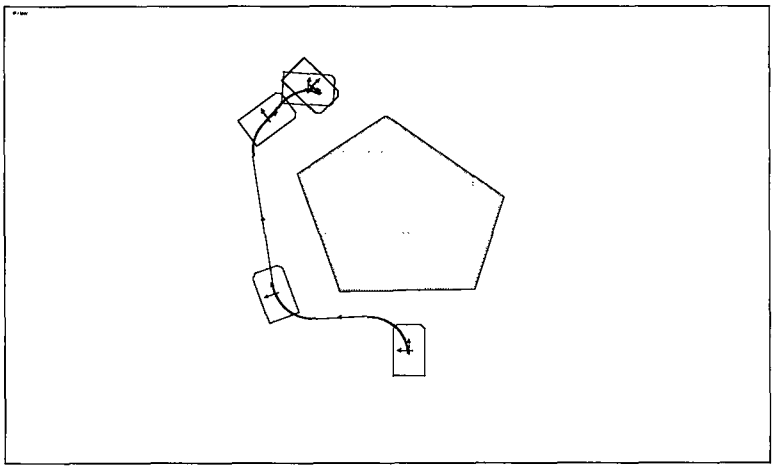

Figure 5: *Pavement with stars.*

From pavements to collision-free feasible paths: By definition of the bubbles, in both pavements the shortest path between the centers of two adjacent bubbles (balls or stars) is collision-free. Then the sequence of the shortest paths linking iteratively the centers of adjacent bubbles constitutes a collision-free feasible path, i.e. a solution to the nonholonomic path planning problem.

Complexity of the pavements: We define the complexity of a pavement by its number of bubbles. This notion is closely related to the complexity of the nonholonomic motion planning problem.

While in classical (holonomic) path planning, the complexity of the problem only depends on the complexity of both the robot and the environment (e.g., number of polygons edges), it is known that nonholonomy requires to account for the size of the free space. For instance, it has been proved in that the number of maneuvers necessary to park a car between two other ones is in $\Omega(\epsilon^{-2})$ (see Figure 6). This result is a consequence of the shape of the nonholonomic metric in the neighborhood of a configuration. It is derived from a complexity model consisting in paving a path by nonholonomic balls [1, 7], exactly as provided by the first pavement above. Nevertheless this model of complexity accounts only for the worst cases (i.e., when the size of the free space is very small); in such cases the pavement by balls is optimal.

The pavement by stars suggests another model of complexity for nonholonomic path

planning: the complexity of a path is the number of stars necessary to cover it. Figure 7 illustrate the interest of this model: in a corridor the number of balls necessary to cover the straight line segment depends linearly on the length of the corridor, while the solution has clearly a constant cost. The pavement by stars accounts for this constant cost: only one star is necessary.

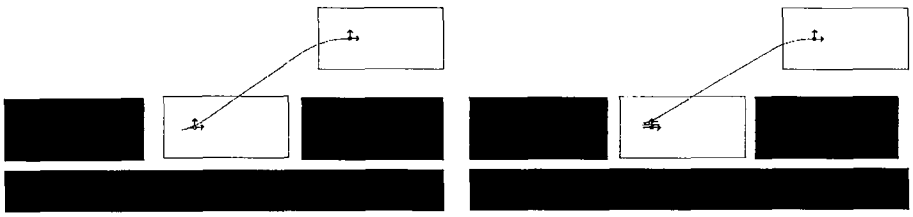

Figure 6: *The number of maneuvers varies as the inverse of the square of the free space.*

In most cases the number of stars used to cover a path is considerably smaller that the necessary number of balls (compare Figures 4 and 5). Due to the inclusion of $\mathcal{B}(C, d_C)$ in $\mathcal{E}(C)$, it is always smaller and it is equivalent for the worst cases.

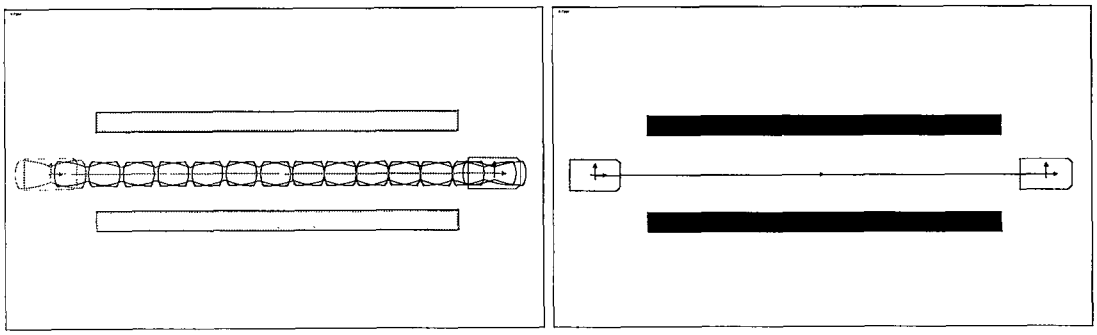

Figure 7: *A ball band and a star band in a corridor.*

Note: The algorithms above assume that the initial path has been firstly sampled into a sequence of l configurations. Then their complexity depends on l. It seems that another way to build both pavements would consist in directly computing the intersection of σ with the balls and the stars respectively. The shape of the balls and the shape of the stars can be analytically computed (see Figures 1 and 2). It remains that their frontier is too complex to hope for exact intersection algorithms even with simple curves such as lines.

An alternative way to build a pavement by stars can be done by using a dichotomy procedure as it appears in the approximation step of the nonholonomic path planner described in [7]. We first try to reach the goal directly from the initial configuration by the shortest feasible path. If this path intersects an obstacle, the configuration halfway along σ is used as a subgoal. The problem is thus broken into two subproblems. If, at any point, the minimal length path between subgoals is not collision-free, then we recursively subdivide σ. When all of the necessary subdivisions are completed, the stars centered at the intermediate points constitute a pavement of σ. The advantage of this method is to not require any sampling of σ. Nevertheless, experiments shows that the convergence of the algorithm is in general slower than the algorithm above. For instance the planner by dichotomy of the holonomic path of Figure 8 (top) requires 10981 subdivisions (computed in more than 1 minute[1]) while

[1]The holonomic paths presented in this paper have been computed by using the holomonic planner described

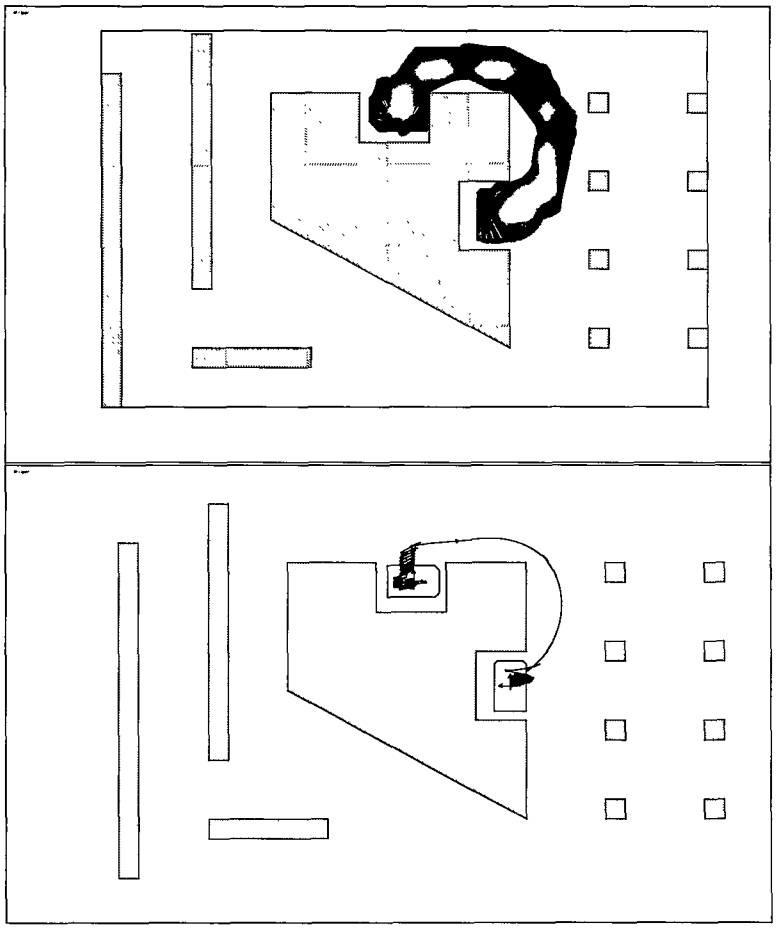

Figure 8: *A holonomic path (top) and the nonholonomic path provided by the star band (bottom)*

our algorithm requires only 500 initial balls which are reduced to 66 stars constituting the band of Figure 8 (bottom). The computation time was 0.8 seconds.

4 Bubble band optimization: elastic band

Once a first pavement created, we consider the associated collision-free feasible path (constituted by a sequence of shortest paths). The path together with its pavement constitutes the so-called bubble band. This section presents a machinery tending to optimize the form and length of the band and allowing to integrate environment changes dynamically.

The basic operations deal with the bubbles: bubbles may be modified individually (by moving their center), new bubbles may be added and redundant bubbles may be removed. In order to guarantee a feasible path, the bubble band must always verify the three following conditions:

- The bubbles should belong to the free space (*non-collision condition*),
- Successive bubbles should be connected (*feasibility condition*),

in [2]. All the algorithms have been implemented and run on a `SPARCstation20`.

- The bubble band should converge in a static environment (*stability condition*).

In [5], the reactivity of the ball band is governed through the balls' centers. This is possible because the balls are close together. This is not true for the star band where stars may be far from each other. Nevertheless, the creation strategy will make it possible to define forces on the star centers and still respect the above conditions. We begin by presenting an energy function that the star band has to optimize. We will show that all the operations applied to the band tend to minimize this energy in order to insure the convergence of the band.

Two configurations C_1 and C_2 being given, we denote by $\gamma(C_1, C_2)$ the shortest path between them. The length of $\gamma(C_1, C_2)$ is $d_{RS}(C_1, C_2)$. $\mathsf{clear}(\gamma)$ is the (Euclidean) distance between a path γ and the obstacles. Let $\mathfrak{BE} = \{\mathcal{E}_i(C_i), i = 1, \ldots, n\}$ be a star band.

The energy is composed of two terms:

$$\mathcal{P}(\mathfrak{BE}) = \mathcal{P}_{\text{int}}(\mathfrak{BE}) + \mathcal{P}_{\text{ext}}(\mathfrak{BE}). \tag{1}$$

The first, called the internal energy, is proportional to the length of the band (i.e., the length of the associated path):

$$\mathcal{P}_{\text{int}}(\mathfrak{BE}) = A \sum_{i=1}^{n-1} d_{RS}(C_i, C_{i+1}). \tag{2}$$

The second term is proportional to the distance to obstacles and, consequently, is called the external energy:

$$\mathcal{P}_{\text{ext}}(\mathfrak{BE}) = B \min_{i=1,\ldots,n-1} u(\mathsf{clear}(\gamma(C_i, C_{i+1}))), \tag{3}$$

where u is a positive convex derivable function whose domain (i.e. the interval on which its value is not equal to zero) is some interval $[0, d_{\min})$; $d_{\min}$ represents the limit of the obstacles influence. For example,

$$u(d) = \begin{cases} (d - d_{\min})^2 & \text{if } \text{dis}_{\mathcal{O}}(P, \mathcal{O}) < d_{\min}, \\ 0 & \text{otherwise.} \end{cases}$$

We begin by presenting the operations of creating new bubbles and removing unnecessary ones. Then we will study the forces that are applied to the bubble centers.

4.1 Connectivity

In order to respect the accessibility condition, a star should be created between two successive stars before they become disconnected.

Let $\mathfrak{BE} = \{\mathcal{E}(C_i), i = 1, \ldots, n\}$ be a connected star band. If $\mathsf{clear}(\gamma(C_i, C_{i+1}))$ becomes lesser than some threshold ϵ, we suppose that the two stars tend to get disconnected from one another. A configuration $C_{i+\frac{1}{2}}$ is then chosen on the path $\gamma(C_i, C_{i+1})$ to be the center of a new intermediate bubble.

Any configuration can be chosen on the path without modifying the band energy since the resulting path is not modified. If $C_{i+\frac{1}{2}}$ is not the closest configuration to the obstacles, either $\gamma(C_i, C_{i+\frac{1}{2}})$ or $\gamma(C_{i+\frac{1}{2}}, C_{i+1})$ will be as close to the obstacles as $\gamma(C_i, C_{i+1})$ and another bubble would then be created. In order to avoid this loop, we choose the new center to be the closest configuration on the original path to the obstacles and we forbid the creation of a new center if its distance to one of the surrounding ones is lesser than its distance to obstacles.

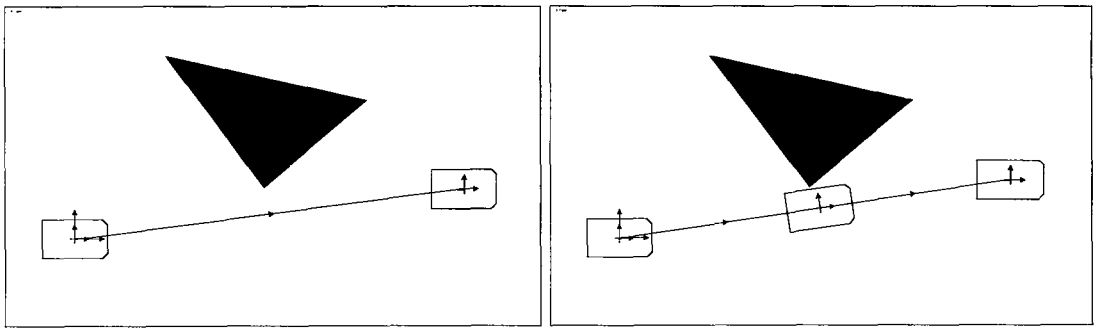

Figure 9: *Creation of a new star.*

To do this, the collision checker of the polygonal robot along the shortest path (described in [7]) has been revisited to provide the configuration closest to obstacles (in case of non-collision).

4.2 Redundancy

A star is no longer necessary whenever its two neighbors become connected. It should then be eliminated. Of course this elimination should not increase the energy of the band.

The elimination of a star reduces the length of the band and the internal energy decreases. On the other hand the resulting path may get closer to obstacles with a consequent increase in the external and maybe in the total energy of the band. In order to avoid this, a star is eliminated if and only if the adjacent bubbles become connected and if the center of the redundant star is close to the path between them.

Not only the creation and elimination operations does not increase the total energy, but also they does not produce a discontinuity in the behavior of the resulting path.

Note that the complexity of both operations is $O(nb)$ where n is the number of line segments that compose the obstacles and b is the number of bubbles in the band. In fact in the connectivity test the distance between configurations is computed $b-1$ times whereas the distance to obstacles is computed $b-1$ times in the redundancy elimination.

4.3 Potentials and forces

The internal structure of the bubble band is always the same whatever shape the bubbles take. It can be thought of as a sequence of configurations successively joined together by shortest paths which belong to the free space. The union of these paths form the global path that connect the start configuration to the goal.

The contraction force between two consecutive bubbles is taken to be the negative gradient of the internal energy.

To avoid obstacles, a force should be exerted on the stars for the global path to move away from them. Since the closest configurations to the obstacles on local paths are centers of stars (or else they are far from obstacles and not affected by them), it is sufficient to apply a repulsive force on these centers to obtain the desired result.

The sum of both forces makes the band move in the direction of energy decreasing. At each sampling step bubbles are created (to guarantee the connectivity) or removed. We have seen that these operations do not modify the total energy of the band. Then the energy of the band is always decreasing (it cannot oscillate). The three conditions (non collision, feasibility, and stability) are satisfied.

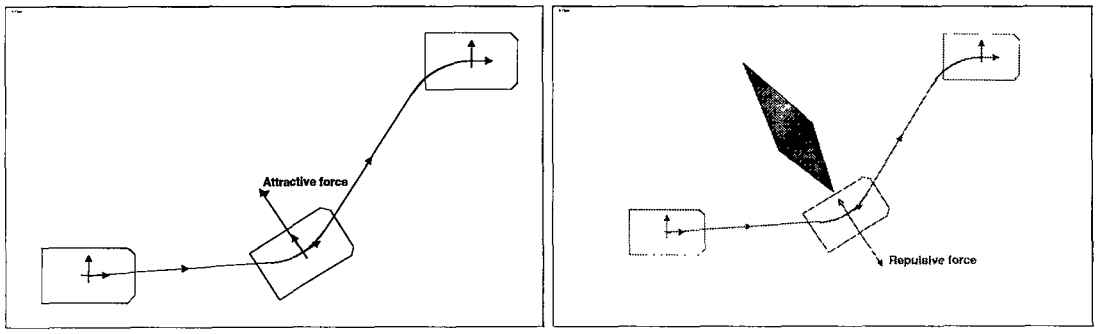

Figure 10: *Internal and external forces.*

Finally, the complexity of the force computation and application is the same as that of bubble creation and elimination. While $b-1$ operations are necessary to compute the gradient of the $b-1$ local distance between centers, nb operations are necessary to compute the distance to obstacles. The total complexity is thus $O(nb)$.

4.4 Comments

Both balls and star bands optimization routine have been implemented. Two comments may be illustrated by Figures 11 and 12.

- The path associated to the minimum energy does not correspond to a minimal length shortest path in the presence of obstacles. This is only a "good" path making a compromise between minimal length and optimal clearance. Indeed the optimization routine above depends on the value of the constant real numbers A and B appearing in equations (2) and (3). The value of B for the solutions appearing in Figures 11 and 12 on the left is greater than the value used to compute the solutions appearing on the right.
- The same figures illustrate the interest of the stars with respect to the balls. In the case of balls, for the path length to decrease, the band is sometimes forced to get close to obstacles. The balls become then smaller and their number increases (from 8 to 11 in Figure 11). This incompatibility between length and number of bubbles is less important in the case of stars, mainly because the stars are not bounded in diameter as are the balls (the number of stars remains constant in the examples shown in Figure 12).

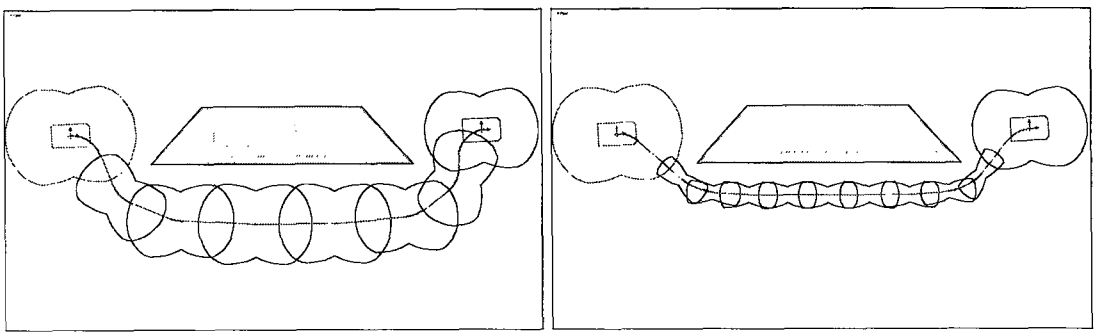

Figure 11: *Number of balls versus length of paths.*

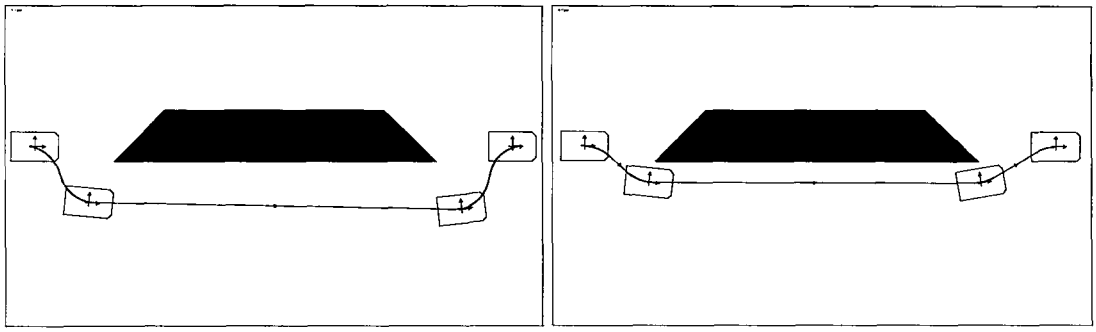

Figure 12: *Number of stars versus length of paths.*

5 Applications

Two main applications of the star bands are possible.

Holonomic path approximation: It is well known that car-like robots are small-time controllable (for any bounded domain of the free space, from any starting configuration lying in this domain, there exist a neighborhood of the starting configuration whose points are reachable without leaving the domain); as a consequence, any holonomic collision-free path can be approximated by a sequence of collision-free feasible paths. This idea is at the origin of the planner described in [7]. The elastic band appears as a good method for devising approximation routines. For instance we have seen that we can control the clearance to the obstacles just by tuning two parameters. Moreover the method is fast: the solution computed for the example in Figure 13 (bottom) takes 1.09 seconds to approximate and smooth the initial holomonic path (Figure 13, top); it contains just one cusp. Figure 14 shows the smoothing of the first nonholonomic path appearing in Figure 8.

Reactiveness to environment changes: The method is sufficiently fast to allow reactiveness to environment changes. Figure 15 (top left) shows a first path provided by the application of the star band (the intermediate positions correspond to the star centers). When we add an unexpected obstacle (black square) the elastic band moves providing a new admissible and collision-free path. The reactiveness of the optimization routine above is sufficient to move the black square with the mouse: the new path is computed in real time. Figure 16 shows another example illustrating the fact that the star band can work in very cluttered environment and can generate automatically maneuvers when needed. If the black square would continue to move in the same direction, there would be no more solution: this event is detected by the elastic band method when the creation of a new star becomes impossible.

6 Conclusion

We have seen that the dynamic property of the stars bands presented in this paper allows to improve the capacity of any existing path planner by accounting for the clearance to the obstacles and environment changes. This property may be also exploited during the motion execution phase.

Such exploitation is currently under study on the mobile robot Hilare 2 developed at LAAS-CNRS. It should replace the application of the balls band in this context, as it has been described in [6]. The main interest of the application of the bubble bands in execution

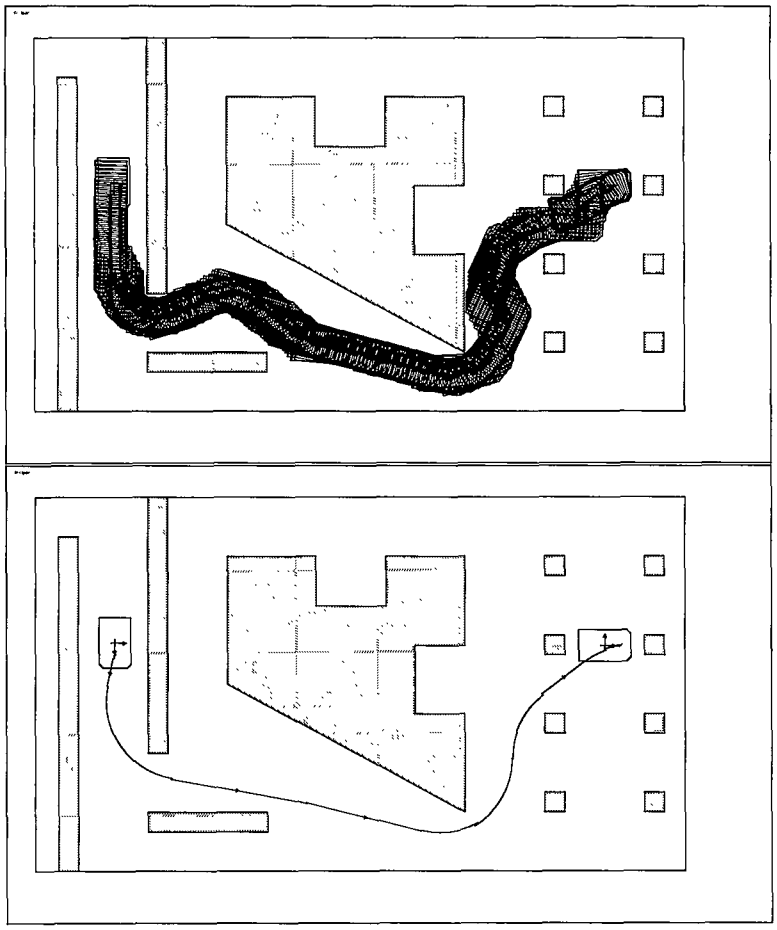

Figure 13: *Smoothing a holonomic path with the elastic band*

phase is twofold: it allows to absorb the uncertainties on both the real environment (w.r.t. to its geometric model) and the real motion; moreover it allows to take into account in real time unexpected moving obstacles (whose dynamics should be of course at the same scale as those of the band).

The algorithmic issue that remains to be explored to improve the method concerns the computation of the shortest paths to the obstacles for a *polygonal* robot.

From a formal point of view, the pavement of paths by (nonholonomic) stars opens new instances of classical problems, such as the art gallery problem: how many car-like robots are necessary to cover a given space ?

Finally we have seen that the number of stars covering a given path gives a better complexity model of the nonholonomic paths than the balls computed in the singular metrics. How this model can be extended to more general nonholonomic systems ?

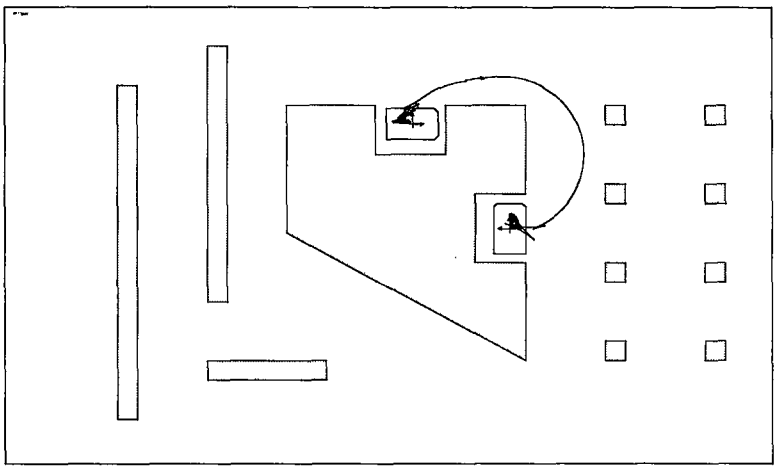

Figure 14: *Smoothing of the path in Figure 8 with the elastic band*

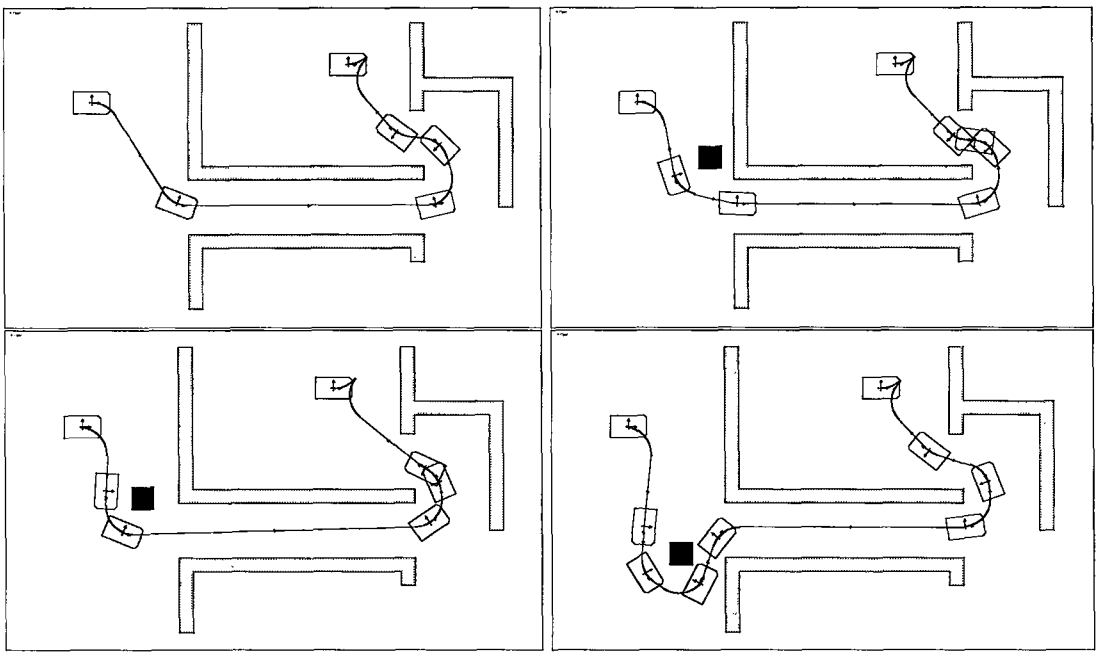

Figure 15: *Reactiveness to unexpected obstacles*

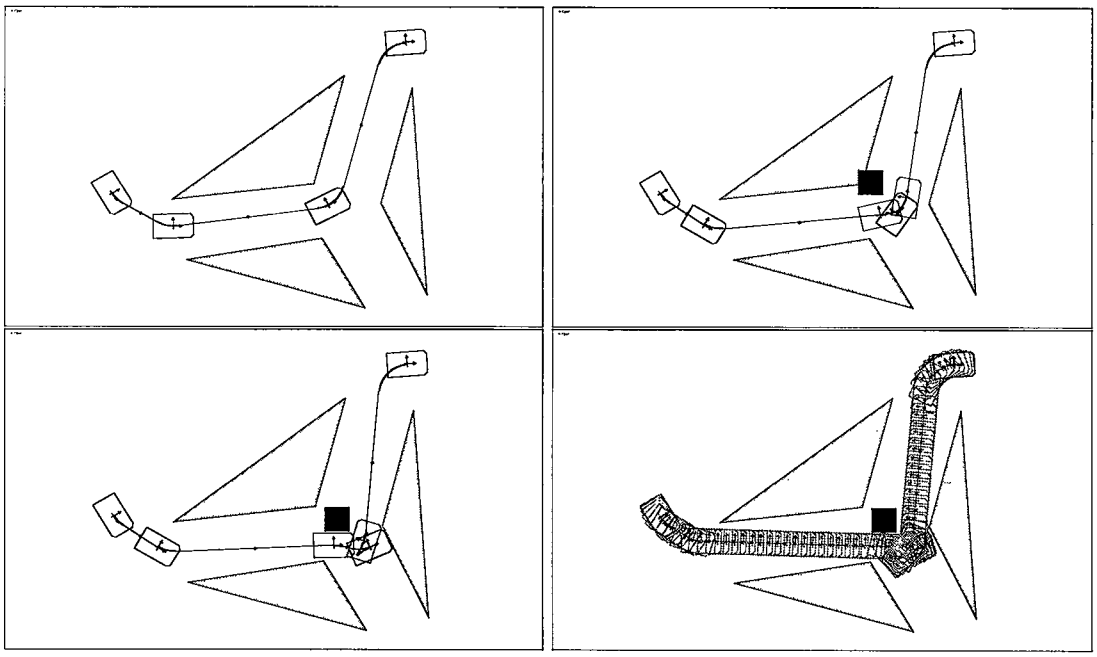

Figure 16: *Reactiveness to unexpected obstacles*

References

[1] A. Bellaïche, J.P. Laumond, and P. Jacobs. Controllability of car-like robots and complexity of the motion planning problem. *International Symposium on Intelligent Robotics*, pages 322–337, 1991.

[2] J. Barraquand, and J.C. Latombe Robot motion planning: a distributed representation approach. *International Journal of Robotics Research*, 1991.

[3] J.D. Boissonnat, A. Cerezo, and J. Leblond. Shortest paths of bounded curvature in the plane. In *IEEE, International Conference on Robotics and Automation, Nice (France)*, pages 2315–2320, May 1992.

[4] H. Jaouni. *Étude d'une métrique non-holonome et applications aux robots mobiles.* PhD thesis, Université Paul Sabatier, December 1997.

[5] M. Khatib, H. Jaouni, R. Chatila, and J.P. Laumond. Dynamic path modification for car-like non-holonomic mobile robots. In *IEEE, International Conference on Robotics and Automation, Albuquerque (USA)*, pages 2920–2925, April 1997.

[6] M. Khatib, H. Jaouni, R. Chatila, and J.P. Laumond. How to implement dynamic paths. In *5th International Symposium on Experimental Robotics, Barcelone (Espagne).*, pages 225–236, June 1997.

[7] J.P. Laumond, P. Jacobs, M. Taix, and R. Murray. A motion planner for non-holonomic mobile robot. *IEEE, Transactions on Automatic Control.*, 10, 1994.

[8] S. Quinlan. *Real-Time Collision-Free Path Modification.* PhD thesis, Stanford University, CS Departement, January 1995.

[9] S. Quinlan and O. Khatib. Elastic bands: connecting path planning and control. In *IEEE, International Conference on Robotics and Automation, Atlanta (USA)*, 1993.

[10] J.A. Reeds and L.A. Shepp. Optimal paths for a car that goes both forwards and backwards. *Pacific Journal Mathematics*, 145(2):367–393, 1990.

[11] P. Souères, J.Y. Fourquet, and J.P. Laumond. Set of reachable positions for a car. *IEEE, Transactions on Automatic Control.*, 39(8), August 1994.

[12] P. Souères and J.P. Laumond. Shortest paths synthesis for a car-like robot. *IEEE, Transactions on Automatic Control.*, 41(5), May 1996.

[13] H.J. Sussmann and W. Tang. Shortest paths for the reeds and shepp car: a worked out example of the use of geometric techniques in nonlinear optimal control. Technical Report SYSCON-91-10, Rutgers Center for systems and Control, 1991.

[14] M. Vendittelli and J.P. Laumond. Visible position for car-like robot amidst obstacles. In *Algorithms for Robotic Motion and Manipulation, 1996 WAFR*, J.P. Laumond and M. Overmars Eds, A.K. Peters, 1997.